

DIFFUSION OF LITHIUM IN THE TiO₂ CATHODE OF A LITHIUM BATTERY

K. KANAMURA, K. YUASA and Z. TAKEHARA

Department of Industrial Chemistry, Faculty of Engineering, Kyoto University, Yoshidahommachi, Sakyo-ku, Kyoto 606 (Japan)

Summary

The diffusion coefficient of lithium in various types of TiO₂ has been investigated by a potential-step method. The TiO₂ electrodes were prepared by rf sputtering to simplify the diffusion behavior of lithium. It has been found that increase in the crystallinity of anatase TiO₂ retards the diffusion of lithium in this material and that the diffusion in rutile TiO₂ is slower than that in anatase TiO₂.

Introduction

Lithium non-aqueous cells have been investigated with a view to the production of high-energy-density batteries. Metal oxides and metal sulfides having channel or layer structures have been proposed as the cathode active material for lithium non-aqueous cells [1 - 3]. The discharge reaction of such cells proceeds via the insertion of lithium into the cathode active material. This process involves the diffusion of lithium into the solid phase. Therefore, a study of the diffusion behaviour of lithium in the active material is most important for the further development of these lithium cells and batteries.

In this study, TiO₂, which has a channel structure, was chosen as the cathode active material [4]. Thin films of anatase and rutile TiO₂ were deposited on a gold substrate by rf sputtering [5] in order to achieve a uniform thickness and to avoid complications, for example the effect of diffusion in the pores and the contribution of spherical diffusion, caused by using electrodes made from active-material powder. The diffusion behaviour of lithium in TiO₂ was studied using a potential-step method. The effect of the crystallinity of the TiO₂ thin film on the rate of diffusion of lithium was also examined.

Experimental

Preparation of TiO₂ thin films

An rf (13.56 MHz) sputtering system was used to deposit the films. The pressure in the sputtering chamber was reduced to 1.0×10^{-7} Torr prior

to the deposition process. The substrate was a nickel plate onto which gold was deposited by d.c. sputtering. The sputtering gas was an 80/20 mixture of argon and oxygen, and the rf power was 60 W. The anatase TiO_2 thin film was deposited from a sintered TiO_2 target (dia.: 80 mm) at a pressure of 1.0×10^{-1} Torr for 15 h. The same target material was used for preparation of the rutile TiO_2 thin film; the target diameter was 60 mm, the pressure 5.0×10^{-2} Torr, and the reaction time 17 h. The temperature of the substrate was maintained at 400 °C during the deposition of the films. The thickness of each film was estimated from the difference in weight before and after deposition, and was also obtained from scanning electron microscopic (SEM) examination of the film cross-section. The anatase TiO_2 film was heat-treated at 400 °C for 20 h in air in order to increase its crystallinity. The crystal structure of the thin film was determined using an X-ray diffractometer with $\text{Cu K}\alpha$ radiation.

Electrochemical measurement

Titanium oxide thin films were used as the cathode material; the reference and counter electrodes consisted of lithium. The electrolyte was propylene carbonate with 1.0 M LiBF_4 . The TiO_2 electrode was potentiostatically discharged from the initial rest potential to a more negative value, and then held at open circuit until the change in the potential was less than 1 mV h^{-1} . The electrode was then further potentiostatically discharged to a more negative potential. The diffusion coefficient of lithium in TiO_2 was obtained from the current-time transient during the potentiostatic discharge, assuming a one-dimensional finite diffusion of lithium in the TiO_2 film.

Results and discussion

Analysis of the thin films

Figure 1(a) shows the X-ray diffraction (XRD) pattern of the anatase TiO_2 thin film; there are two peaks at $2\theta = 25.44^\circ$ and 47.84° , corresponding to the (101) and (200) planes, respectively. After heat-treatment of the film at 400 °C for 20 h in air, these two peaks are much sharper (Fig. 1(b)) and, therefore, such heat-treatment has increased the crystallinity of the film. The XRD pattern of the rutile TiO_2 thin film has the five peaks of rutile TiO_2 (Fig. 1(c)).

An electron micrograph of the cross-section of the anatase TiO_2 thin film is shown in Fig. 2. Using this micrograph, the film thickness was estimated to be $1.55 \mu\text{m}$, a value in close agreement with that, namely $1.58 \mu\text{m}$, obtained from the difference in weight (assuming the density of anatase TiO_2 to be 3.84 g cm^{-3}). On the other hand, a difference in the thickness of the rutile TiO_2 film was found for these two methods of determination, *i.e.*, $1.22 \mu\text{m}$ (SEM) and $0.97 \mu\text{m}$ (weight difference).

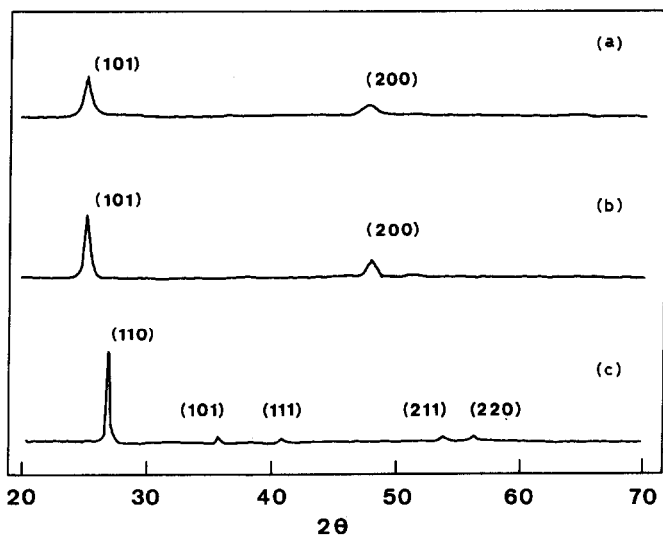


Fig. 1. XRD patterns of TiO_2 thin films; (a) non-heat-treated anatase TiO_2 ; (b) heat-treated anatase TiO_2 ; (c) rutile TiO_2 .

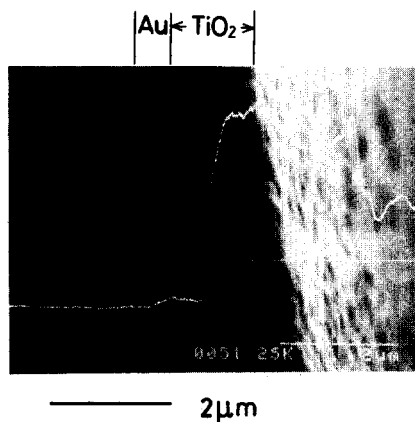


Fig. 2. Electron micrograph of cross-section of anatase TiO_2 thin film prepared by rf sputtering. Film thickness: SEM, $1.55 \mu\text{m}$; mass, $1.58 \mu\text{m}$.

Diffusion coefficient of lithium in TiO_2

It was assumed that the diffusion of lithium in TiO_2 thin film is a simple, one-dimensional, finite diffusion. This assumption was reasonable given the uniformity of the TiO_2 thin film. The theoretical current-time transient during potentiostatic discharge was obtained from Fick's second law of diffusion:

$$\frac{\partial C(x, t)}{\partial t} = D \frac{\partial C^2(x, t)}{\partial x^2} \quad (1)$$

where D is the diffusion coefficient of lithium in TiO_2 . Assuming that the film thickness of TiO_2 is l , initial and boundary conditions are written as follows:

$$C(x, t) = C_0, \quad t = 0, 0 < x < l \quad (2)$$

$$C(x, t) = C^*, \quad t > l, x = l \quad (3)$$

$$\frac{\partial C(x, t)}{\partial x} = 0, \quad x = 0 \quad (4)$$

The theoretical current-time transient is given by:

$$\frac{i(\tau)}{i_\infty} = \frac{1}{\sqrt{\pi\tau}} \left\{ \sum_{n=0}^{\infty} (-1)^n \exp(-n^2/\tau) + \sum_{n=0}^{\infty} (-1)^{n+1} \exp[-(n+1)^2/\tau] \right\} \quad (5)$$

where $i(\tau)/i_\infty$ represents a dimensionless current and τ represents a dimensionless time, i_∞ and τ are given by:

$$i_\infty = nFAD(C^* - C_0)/l \quad (6)$$

$$\tau = Dt/l^2 \quad (7)$$

Figure 3(a) shows the current-time transient during the potentiostatic discharge of a non-heat-treated anatase TiO_2 electrode from the initial rest potential (3.3 - 3.4 V) to 2.0 V. It can be seen that the experimental data deviate from the theoretical curve. On the other hand, there is good agreement for discharge between 2.8 V and 2.0 V, as shown in Fig. 3(b).

For both the heat-treated and untreated anatase TiO_2 electrodes the deviation between the experimental and theoretical curves was observed during discharge from the initial rest potential to 1.5 V, Fig. 4(a). However, the curves coincided during discharge from 2.65 V to 1.5 V in Fig. 4(b).

The above deviation in the current-time transients may be due to the following reasons: First, the TiO_2 thin film used in this study was polycrystalline and therefore has some defects. Lithium diffuses into the grain boundaries as well as into the bulk of the TiO_2 . During the initial period, the discharge appears to proceed via the diffusion of lithium into the grain boundaries rather than into the bulk, namely, the channel, and therefore the observed transient behaviour differs from the theoretical expectation. Second, the deviation may be caused by a change in the electrical resistance of the thin film. In this treatment, it has been assumed that the movement of lithium in TiO_2 is controlled by the diffusion alone. In other words, it is assumed that the transfer of lithium in TiO_2 is much slower than the electron transfer. If the electrical resistance of the TiO_2 thin film is large, then the electron transfer will be comparable with that of lithium diffusion. As a result, lithium not only transfers by diffusion but also by migration. Third,

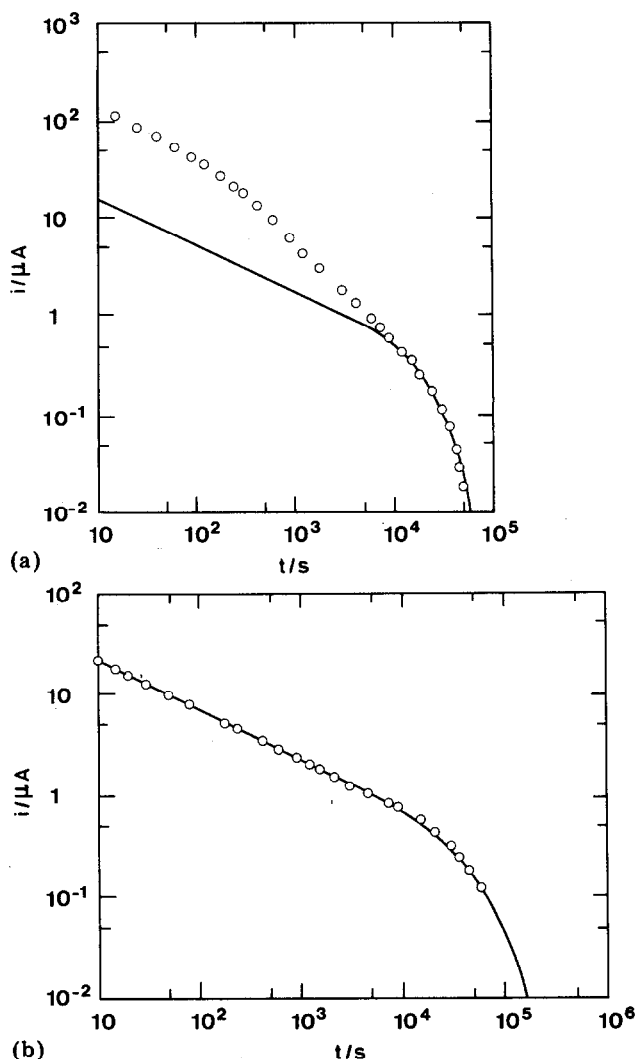


Fig. 3. Current-time transients during potentiostatic discharge of non-heat-treated anatase TiO_2 . (a) From initial rest potential to 2.0 V; (b) from 2.8 V to 2.0 V (O, experimental; —, theoretical curve).

the deviation may be caused by the elastic interaction of inserted lithium atoms. As the insertion of lithium atoms increases, an elastic attractive interaction along the channel will occur [6]. The extent of this interaction changes more extensively during the initial potentiostatic discharge, and therefore the apparent diffusion coefficient of lithium in TiO_2 will decrease with increase in the concentration of lithium in TiO_2 during this period. These factors depend to some degree on the concentration of lithium in the TiO_2 . When this concentration is high, the electronic conductivity of the thin film will also be high because of the formation of Ti^{3+} . Further, the effect

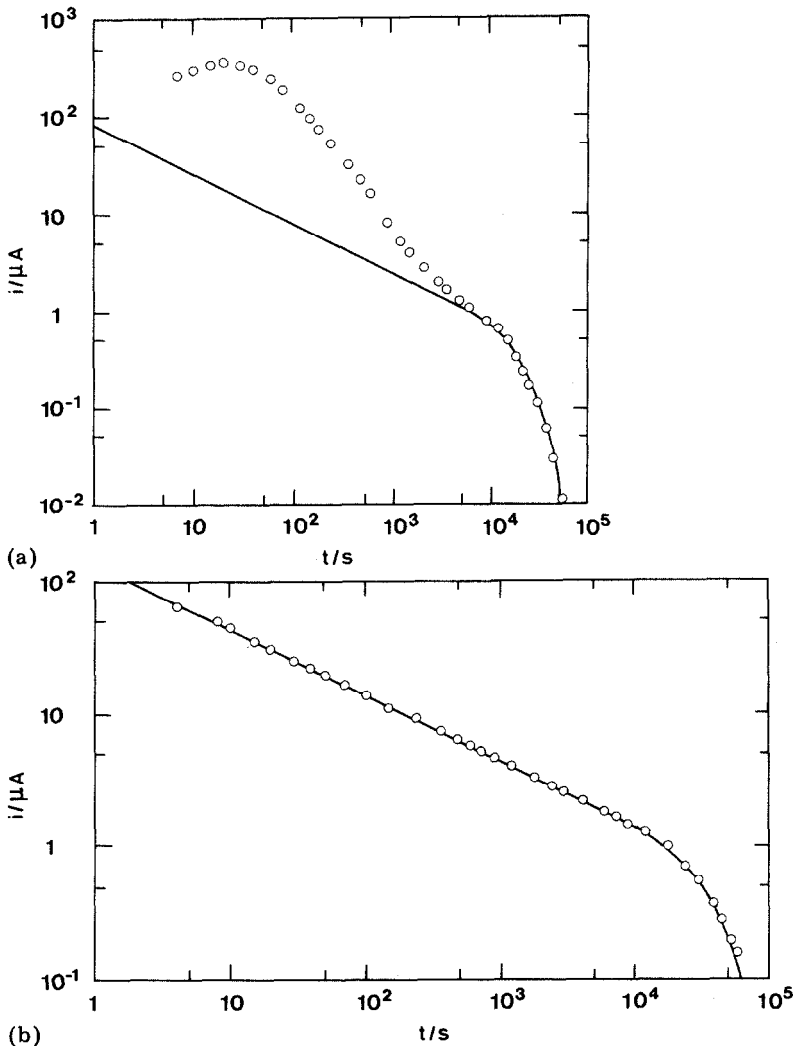


Fig. 4. Current-time transients during potentiostatic discharge of heat-treated anatase TiO_2 . (a) From the initial rest potential to 1.5 V; (b) from 2.65 V to 1.5 V (O, experimental points; —, theoretical curve.)

of TiO_2 defects (e.g., crystal grains) on the diffusion will reduce, since most of the defects will be filled with lithium. The change in the extent of the interaction in TiO_2 after lithium has been inserted is negligibly small during the discharge because the change in the concentration of lithium in TiO_2 is also small. Thus, the apparent diffusion coefficient of lithium in anatase TiO_2 before potentiostatic discharge does not change, and the observed data almost fit the theoretical curve, as shown in Fig. 3(b) and Fig. 4(b). The diffusion coefficient of lithium in the non-heat-treated anatase TiO_2 was estimated to be $3.78 \times 10^{-13} \text{ cm}^2 \text{ s}^{-1}$. On the other hand, for the heat-treated

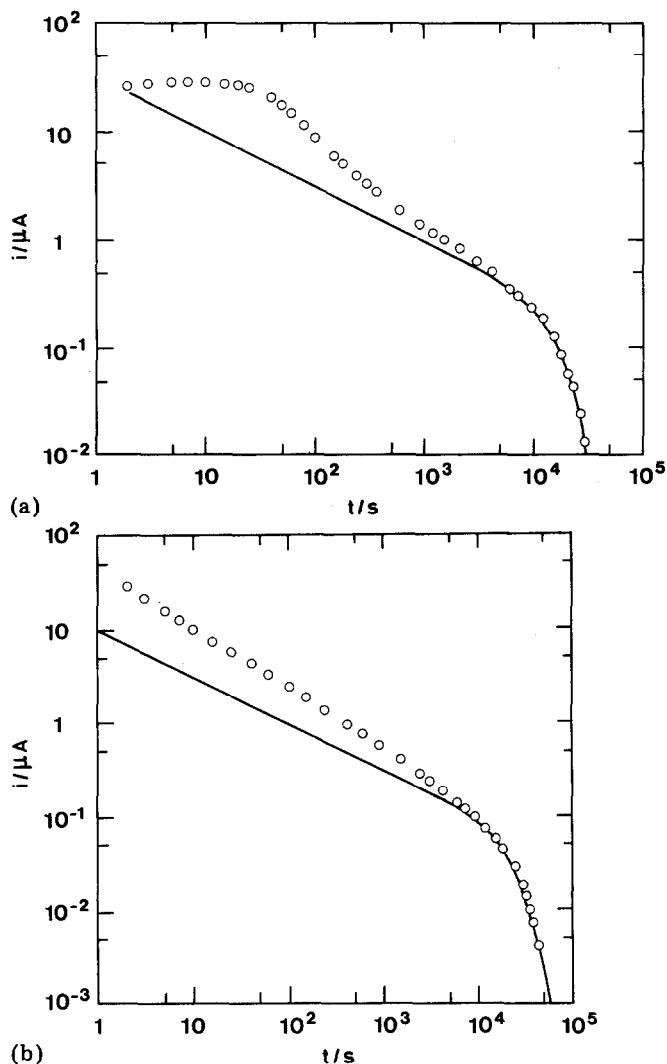


Fig. 5. Current-time transients during potentiostatic discharge of rutile TiO₂. (a) From initial rest potential to 1.5 V; (b) from 2.61 V to 1.5 V (○, experimental points; —, theoretical curve).

anatase TiO₂, the diffusion coefficient of lithium was estimated to be $1.81 \times 10^{-13} \text{ cm}^2 \text{ s}^{-1}$.

Figure 5(a) and (b) presents the current-time transients during the potentiostatic discharge of a rutile TiO₂ electrode from the initial test potential (3.1–3.2 V) to 1.5 V, and from 2.61 V to 1.5 V, respectively. The behaviour of rutile TiO₂ is similar to that of the heat-treated anatase TiO₂. However, unlike anatase TiO₂, discharge of rutile TiO₂ from 2.61 V to 1.5 V (Fig. 5(b)) does not follow the theoretical curve.

The crystallinity of rutile TiO_2 is higher than that of anatase TiO_2 , and the electronic conductivity of rutile TiO_2 is lower than that of anatase TiO_2 . When the concentration of lithium in rutile TiO_2 is high, the electronic conductivity will also be high and the effect of crystal grains on the diffusion will be negligibly small. Therefore, for discharge from 2.61 V to 1.5 V, the deviation between the observed and theoretical values can be attributed to the elastic interaction between inserted lithium atoms. The elastic interaction in rutile TiO_2 is expected to be larger than that in anatase TiO_2 because of the difference in crystal structure. From Fig. 5(b), the diffusion coefficient of lithium in rutile TiO_2 was estimated to be $1.42 \times 10^{-13} \text{ cm}^2 \text{ s}^{-1}$.

Conclusions

The diffusion coefficient of lithium in heat-treated anatase TiO_2 is half that in non-heat-treated anatase TiO_2 . This suggests that an increase in crystallinity retards the diffusion of lithium in anatase TiO_2 . The diffusion coefficient of lithium in rutile TiO_2 is smaller than that in anatase TiO_2 . This is probably due to the fact that the channels of rutile TiO_2 are narrower than those of anatase TiO_2 . These findings indicate that the diffusion behaviour of lithium in TiO_2 is affected both by the crystallinity and by the crystal structure of TiO_2 .

References

- 1 L. Campanella and G. Pistoia, *J. Electrochem. Soc.*, **118** (1971) 1905.
- 2 M. S. Whittingham, *J. Electrochem. Soc.*, **123** (1976) 315.
- 3 G. L. Holleck and J. R. Driscoll, *Electrochim. Acta*, **22** (1977) 647.
- 4 T. Ohzuku, Z. Takehara and S. Yoshizawa, *Electrochim. Acta*, **24** (1979) 219.
- 5 L. C. Wu and J. E. Greene, *J. Appl. Phys.*, **50** (1979) 4966.
- 6 W. R. Mckinnon and R. R. Haering, *Solid State Ionics*, **1** (1980) 111.